P02-08

Geometry dependence of stellarator turbulence via GENE

H.E. Mynick[a], P.Xanthopoulos[b], A.H. Boozer[c], L.Maingi[a], & N.Pomphrey[a]

[a]Princeton Plasma Physics Lab
[b]IPP-MPG, Greifswald
[c]Columbia University

ISHW/ICST Meeting
October 12-16, 19-20, 2009
PPPL, Princeton, NJ

Acknowledgments:
F.Jenko, F.Merz, G.Rewoldt, J.Talmadge, E.Valeo

-Introduction:

- Present day stellarator designs seek to optimize neoclassical (nc) transport. With 3D gyrokinetic (gk) simulation codes like GENE[1,2], one can now seek to characterize and then optimize designs for TOTAL transport.

-Here, we study the turbulence and turbulent transport in a family of configurations, including a representative from each of the main approaches to nc transport optimization, a QA, a QH, a QI/QO, and an axisymmetrized version of the QA, to better understand the geometry dependence of turbulence characteristics in those configurations, and seek to relate the turbulence to key geometric quantities, such as the curvature, local shear, etc.

-Present nonlinear gk stellarator simulations (by GENE, GS2, GKV) are restricted to simulating the plasma only over a flux tube in a specified flux surface. To facilitate our analysis of the turbulent transport, we use a novel procedure, to construct from the 1D (flux-tube) results from GENE the 2D structure of the turbulence over a flux surface.

-Configurations studied here:

-NCSX_sym: Axisymmetrized version of stellarator NCSX.

-NCSX = quasi-axisymmetric (QA) stellarator design. (N_{fp}=3).

-W7X = quasi-isodynamic/quasi-omnigenous (QI/QO) design, now under construction at IPP/Greifswald, Germany. (N_{fp}=5).

-HSX = quasi-helical (QH) design, presently operating at U.Wisconsin. (N_{fp}=4).

NCSX-SYM

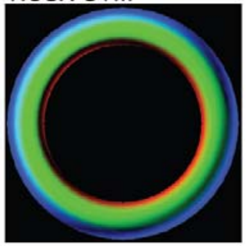

NCSX

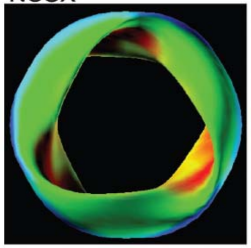

W7-X

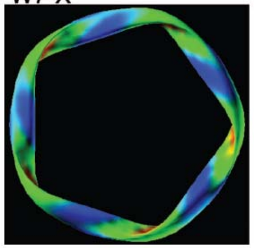

more symmetric ⟷ less symmetric

2D — quasi-symmetric (QS) — fully 3D

			$\varepsilon_h/\varepsilon_t$
NCSX_sym			0
	NCSX (QA)		<<1
	W7X (QI/QO)		~1
	HSX_qhs (QH)	……HSX_mir	>>1

HSX

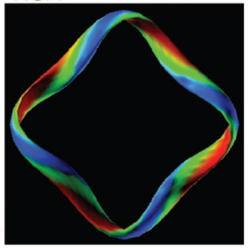

(not yet studied): LHD_inwd (QI/QO)…… LHD_stdd (conventional)

LHD

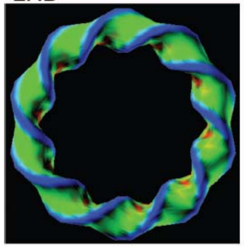

-Coordinate systems:

-Global flux coordinates (ψ, θ, ζ) , with

$\psi \equiv$ toroidal flux/ 2π , or $r(\psi) \equiv (2\psi / B_a)^{1/2}$ =minor radial coordinate,

$\theta, \zeta \equiv$ poloidal & toroidal azimuths, and with reference magnetic field strength B_a.

-Local, flux-tube coordinates (x, y, z) , where

$$x \equiv r - r_0, \qquad y \equiv -r_0 \iota_0 \alpha_t, \qquad z \equiv \theta, \qquad \alpha_t \equiv (\varsigma - q\theta). \tag{1}$$

-Then the magnetic field may be written

$$\vec{B} = \nabla\psi \times \nabla\theta + \nabla\zeta \times \nabla\psi_p = \nabla\alpha_t \times \nabla\psi_p \tag{2}$$

$$= B_a \nabla x \times \nabla y.$$

-Parameters used for runs here:

$$a / L_n \equiv -a\partial_r n / n = 0, \qquad a / L_T \equiv -a\partial_r T / T = 3, \qquad \tau \equiv T_e / T_i = 1,$$

$\rho_s / L_y = \dfrac{.05}{2\pi}, \qquad L_x = L_y, \qquad L_z = 1$ poloidal transit,

with adiabatic electrons, $L_{x,y,z}$=box size in x,y,z-dir'ns, a=avg minor radius.

-Constructing 2D flux-surface picture from ‘1D’ flux-tube quantities:

-Combine results from
N_t tubes 0,1,..N_t-1,

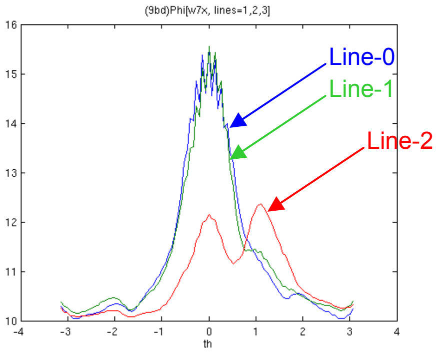

to form picture over
half field-period (fp):

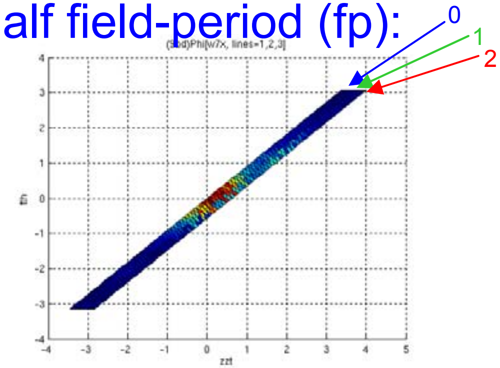

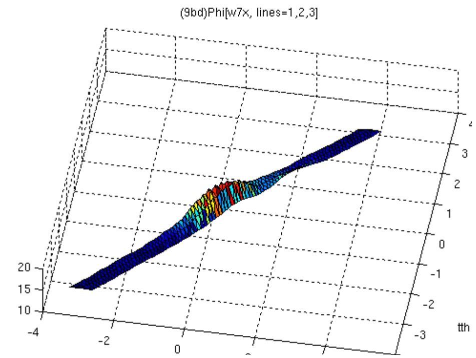

Then, use stellarator symmetry
to construct picture over full fp :

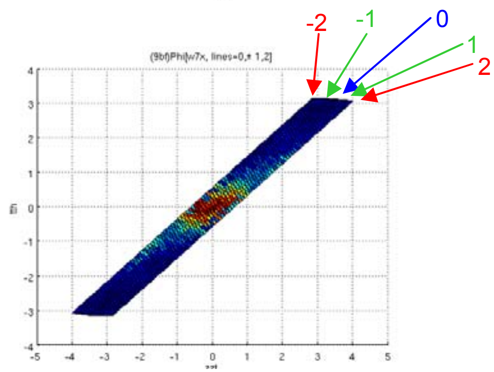

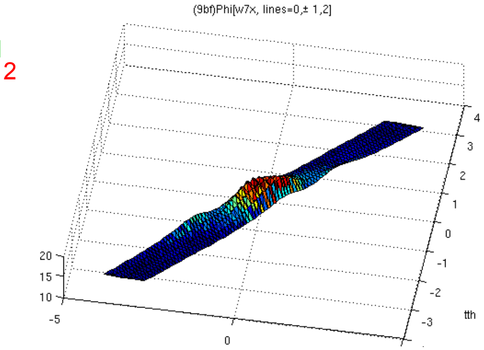

and finally repeat image N_{fp}
times for full flux-surface image:

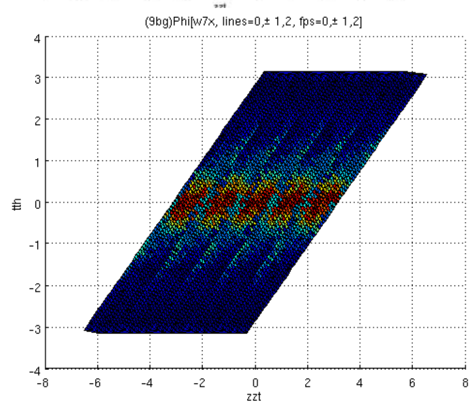

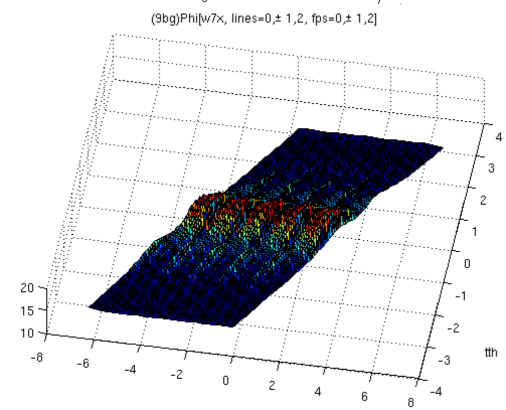

-Fully 2D system: NCSX_sym ($\varepsilon_h/\varepsilon_t=0$) :

-magnetic field strength $B(z) \Rightarrow B(\theta,\zeta)$:

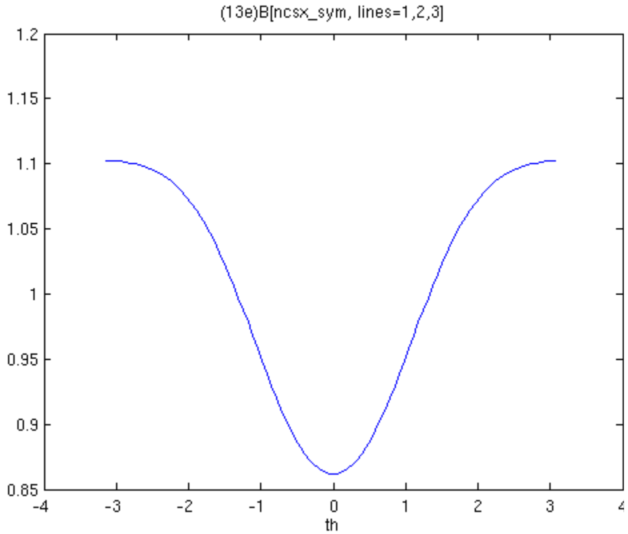

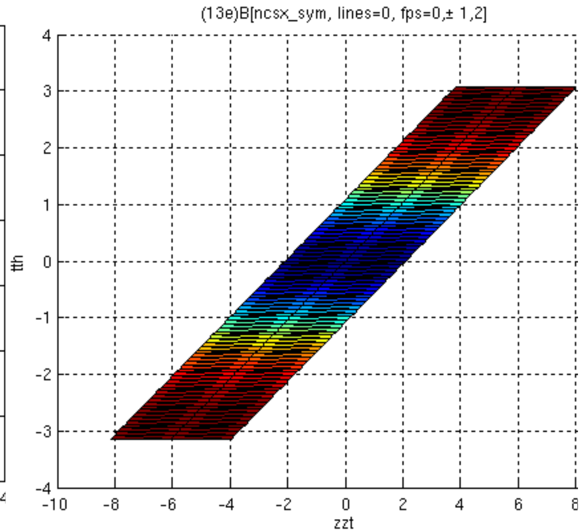

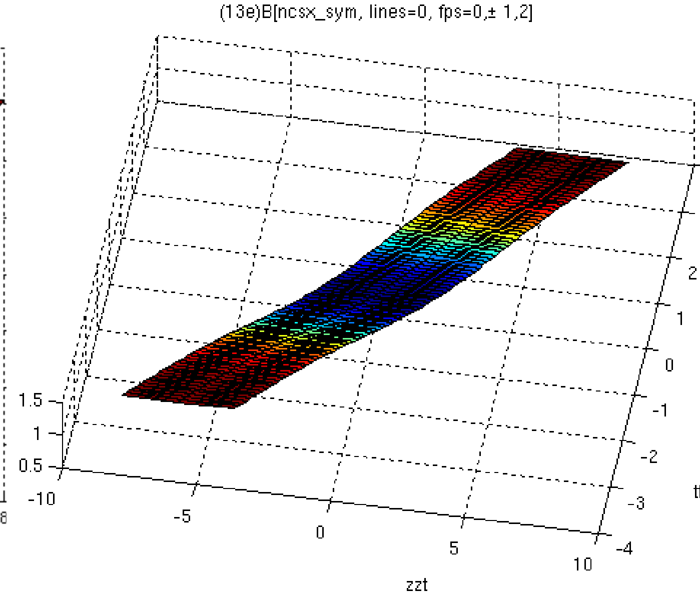

-turbulent amplitude $\langle\varphi\rangle(z) \Rightarrow \langle\varphi\rangle(\theta,\zeta)$:

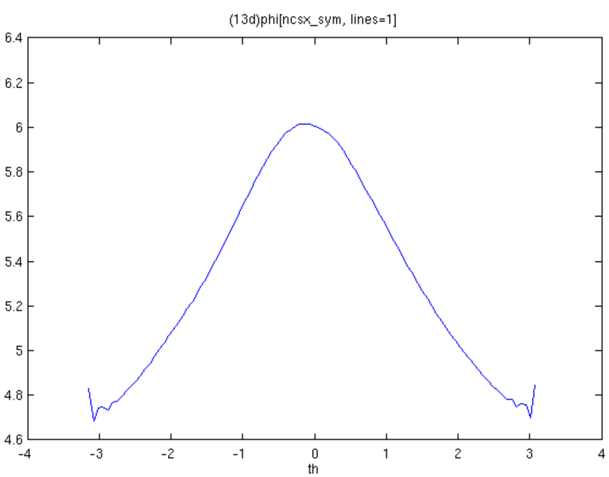

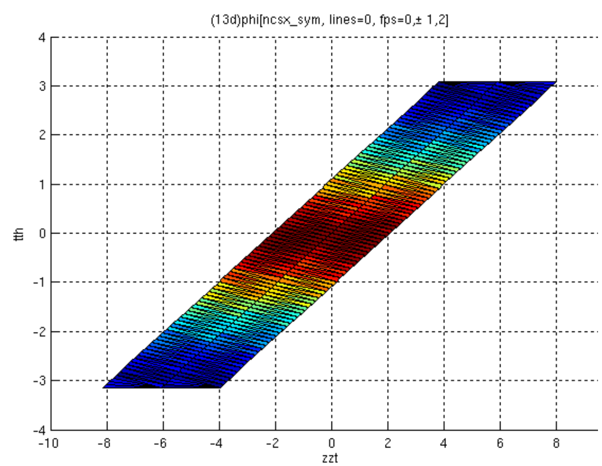

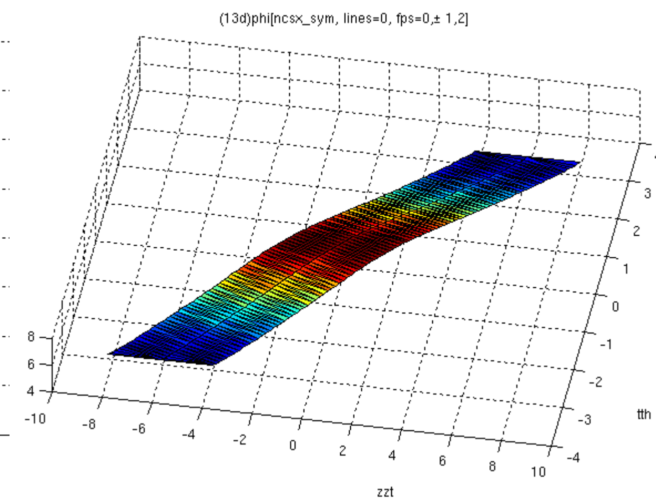

-radial curvature $\kappa_1(z) \Rightarrow \kappa_1(\theta,\zeta), \qquad \kappa_1 \equiv a\partial_r B / B:$

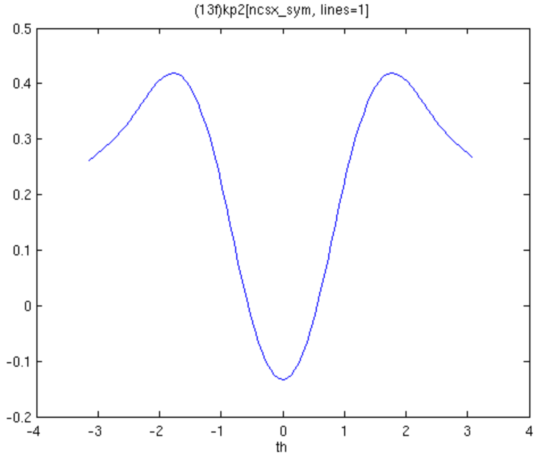

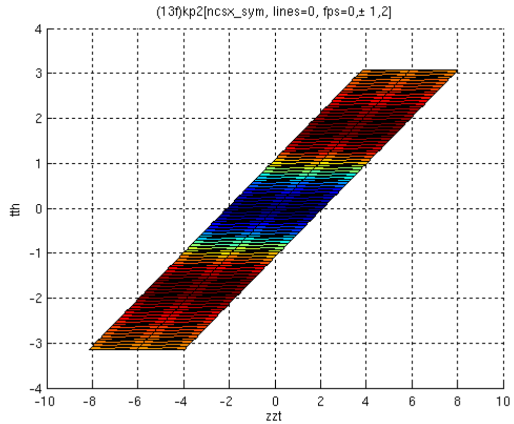

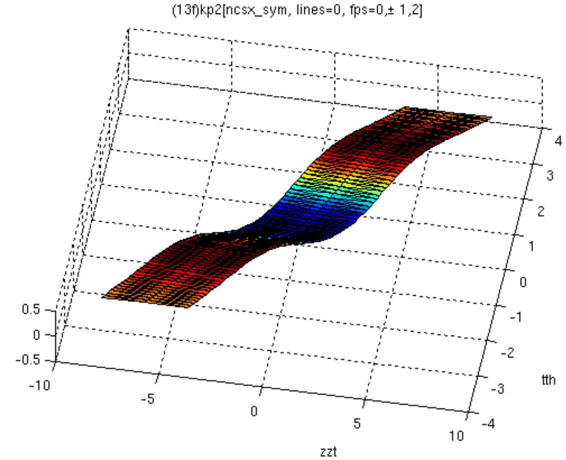

-As expect, <φ> tends to localize in “bad-curvature” (κ_1 <0) regions on outboard side.

-local shear $s_l(z) \Rightarrow s_l(\theta,\zeta), \qquad s_l \equiv J_{\psi_p\theta\alpha}\vec{h}\cdot\nabla\times\vec{h}, \qquad \vec{h} \equiv \vec{B}\times\nabla\psi_p / |\nabla\psi_p|^2:$

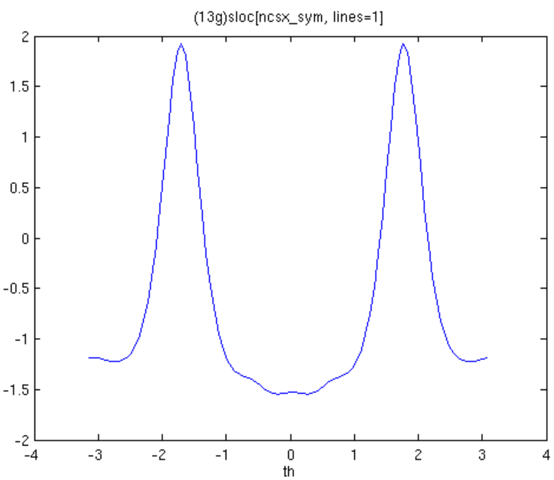

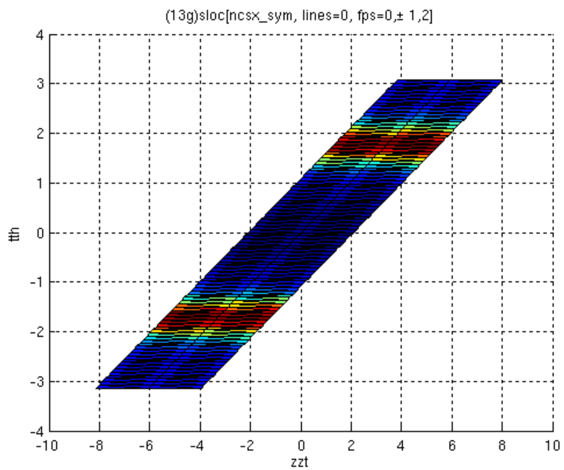

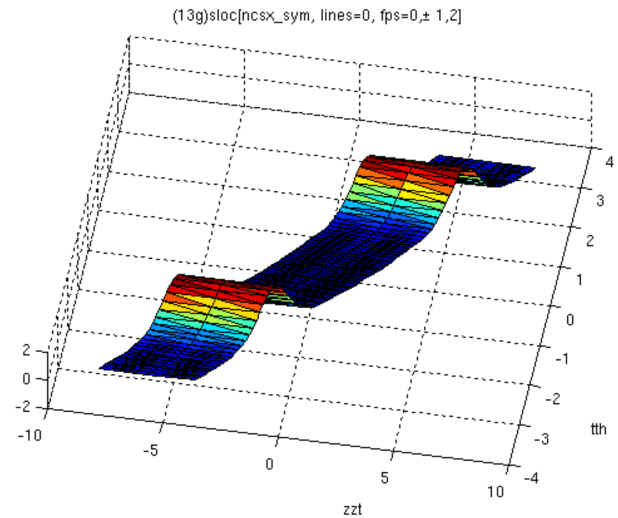

-QA: NCSX ($\varepsilon_h/\varepsilon_t << 1$) :

-magnetic field strength $B(z) \Rightarrow B(\theta,\zeta)$:

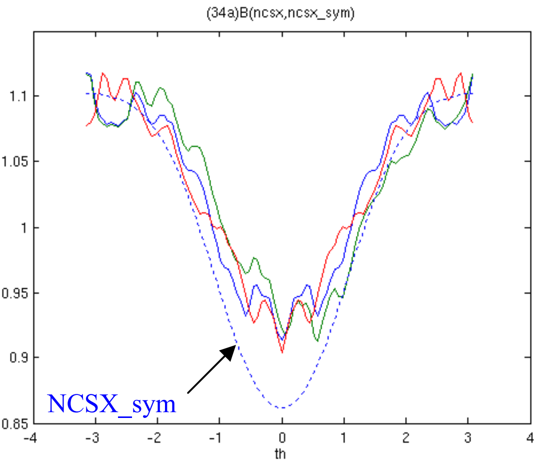

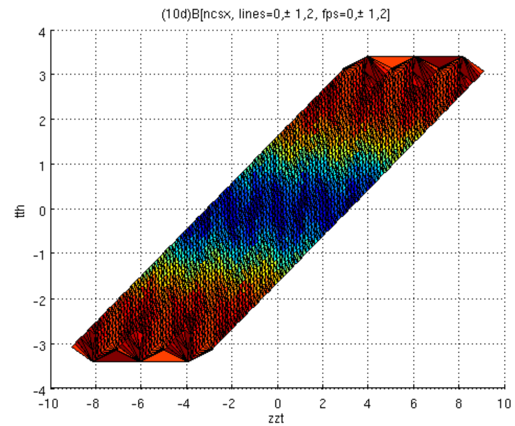

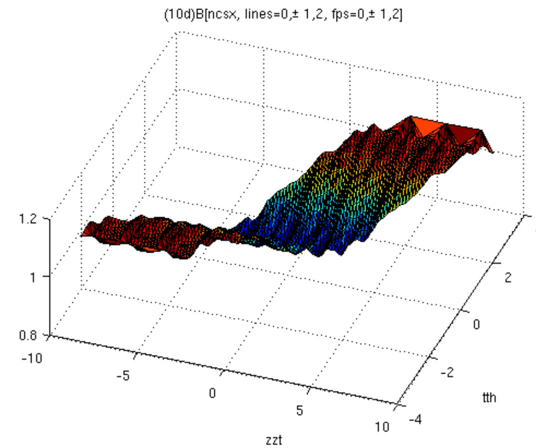

-turbulent amplitude $\langle\varphi\rangle(z) \Rightarrow \langle\varphi\rangle(\theta,\zeta)$:

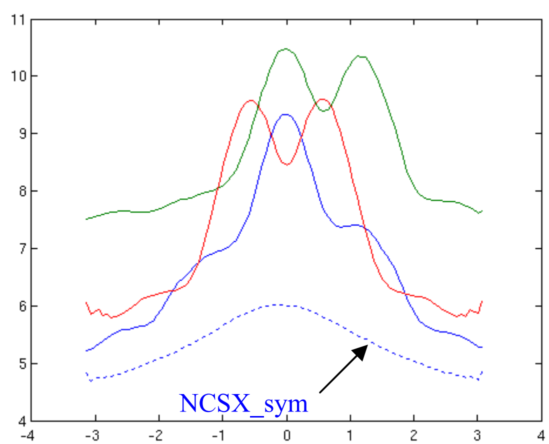

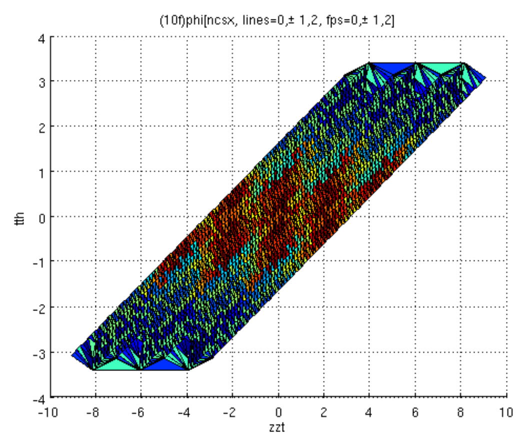

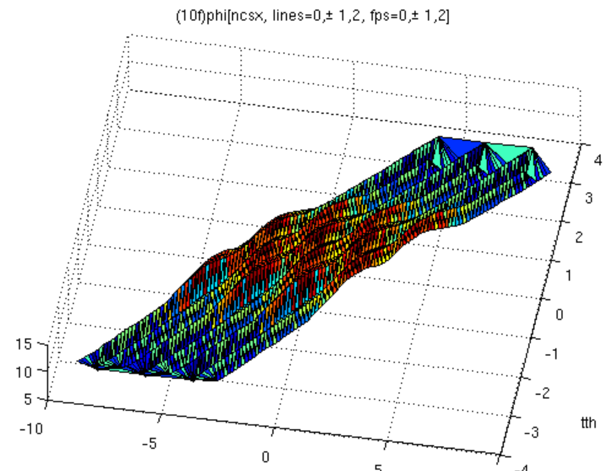

-Physical quantities approximate those in NCSX_sym, modulated by the non-2D imperfections, with the exception of local shear, which is dominated by those imperfections:

-radial curvature κ_1:

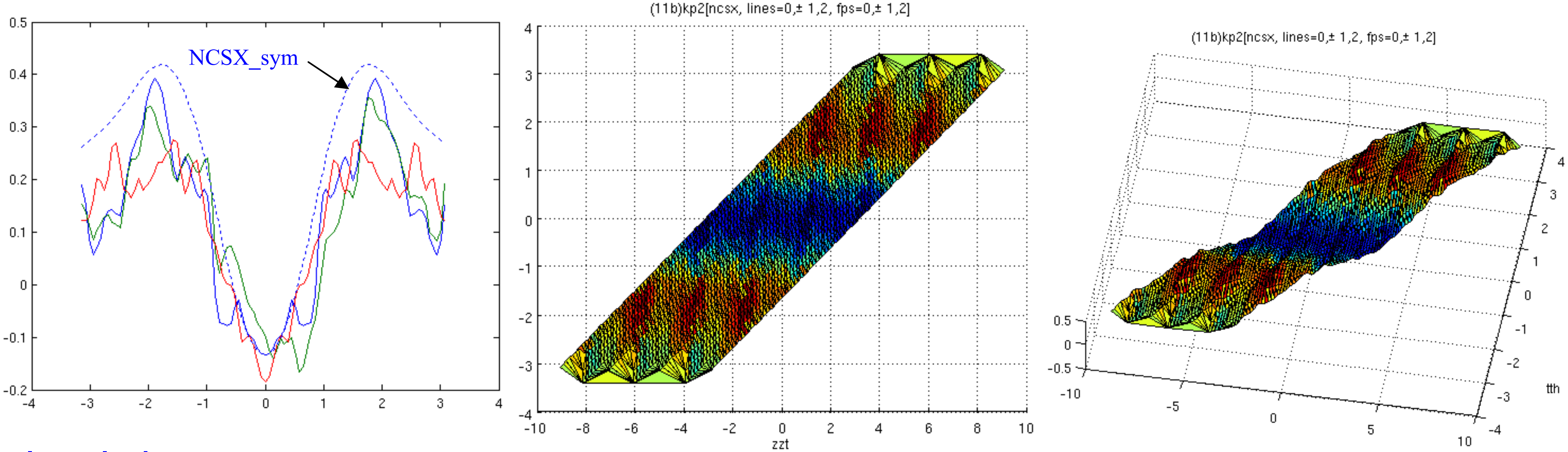

-local shear:

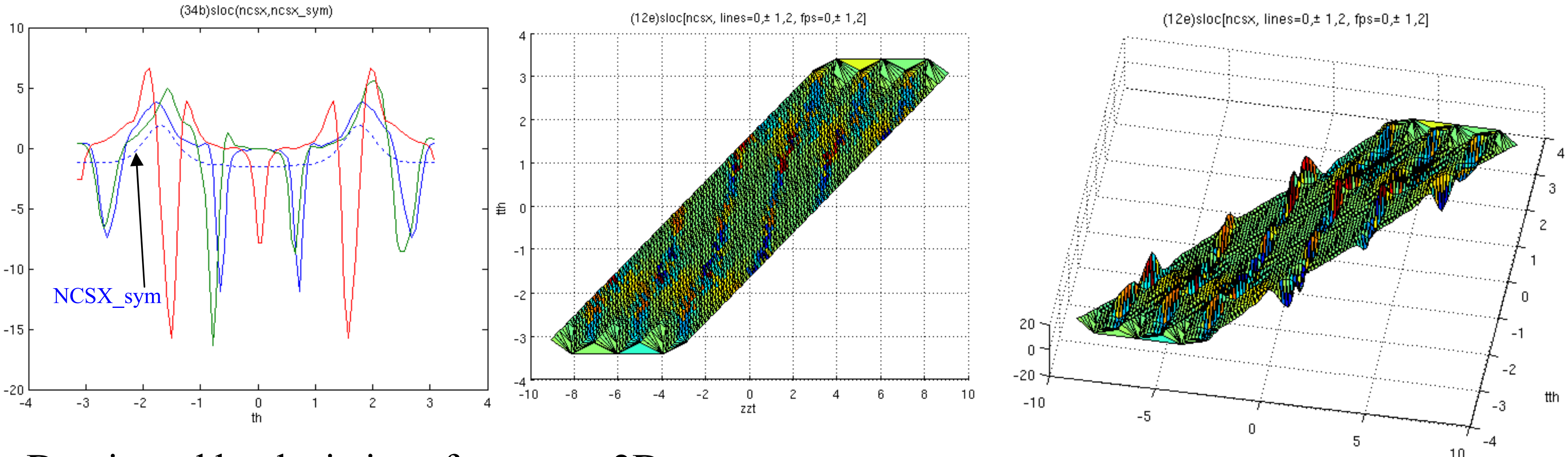

-Dominated by deviations from pure 2D.

-QI/QO: W7X ($\varepsilon_h/\varepsilon_t \sim 1$) :

-magnetic field strength $B(z) \Rightarrow B(\theta,\zeta)$:

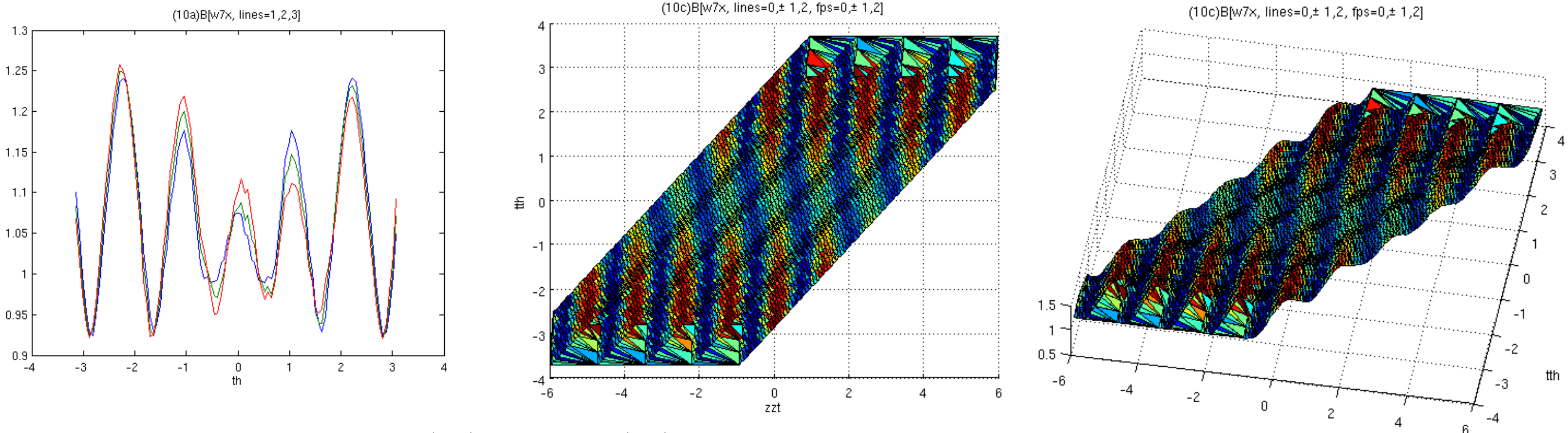

-turbulent amplitude $\langle\varphi\rangle(z) \Rightarrow \langle\varphi\rangle(\theta,\zeta)$:

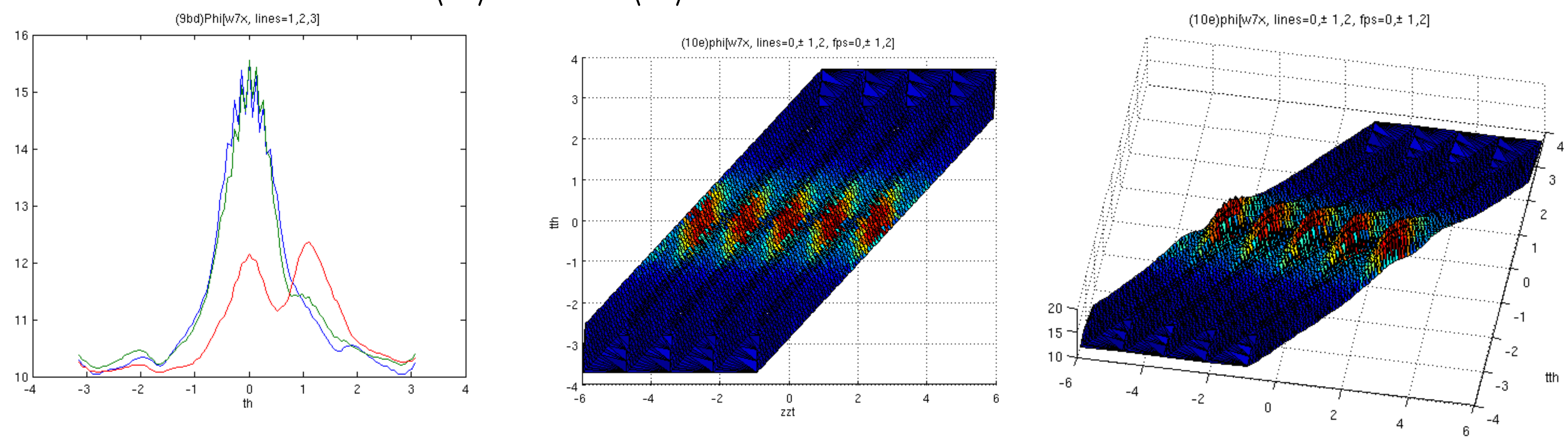

-radial curvature κ_1:

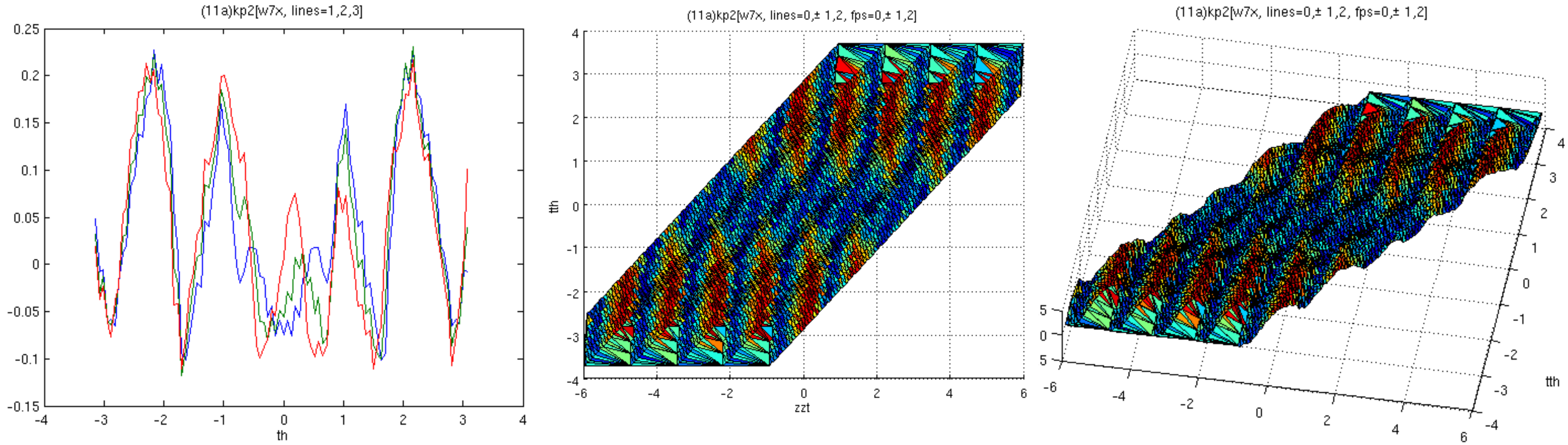

-local shear:

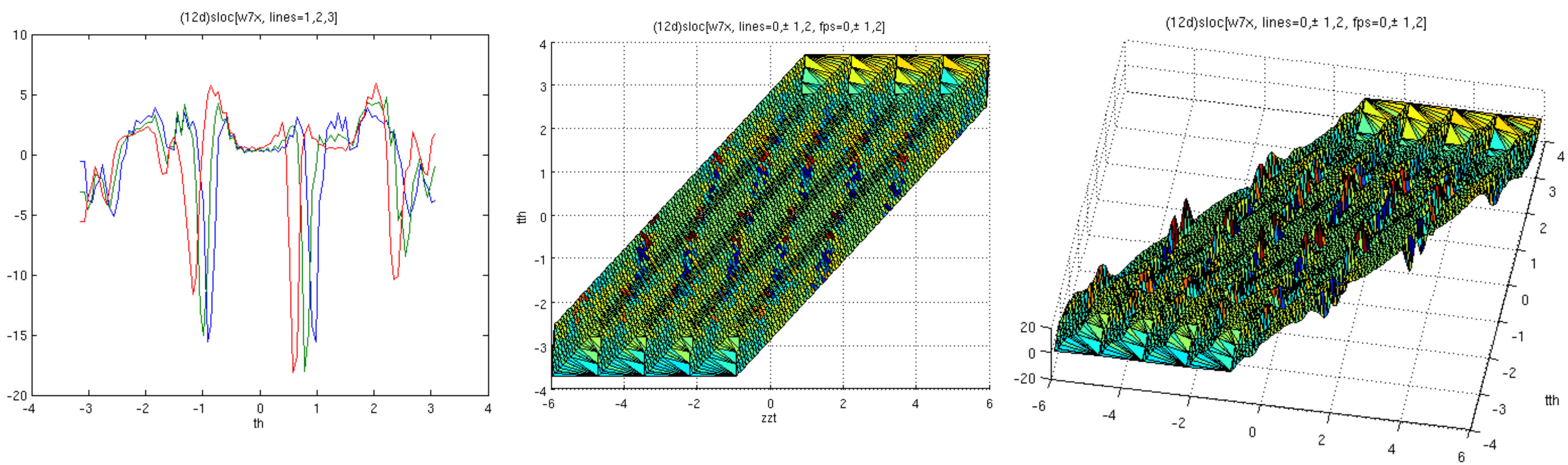

-QH: HSX_qhs:

-magnetic field strength $B(z) \Rightarrow B(\theta,\zeta):$

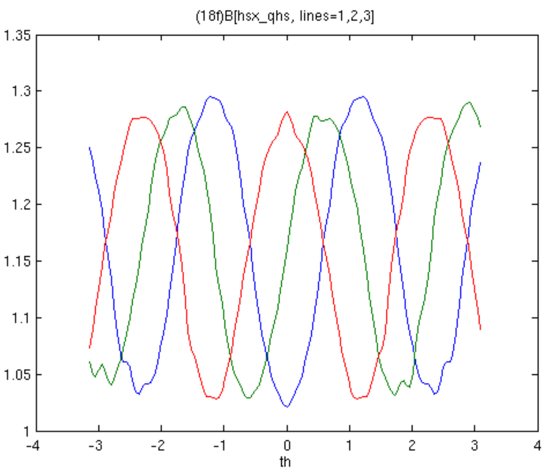

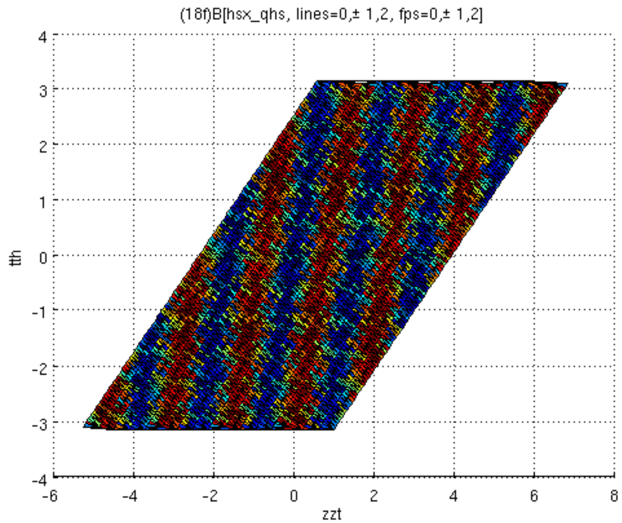

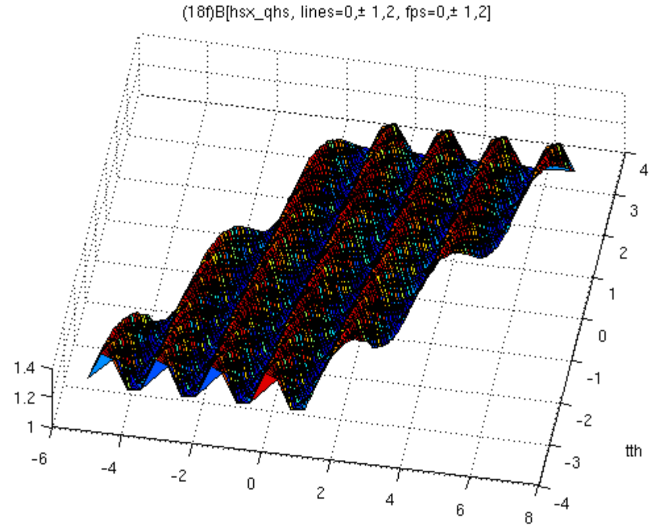

-turbulent amplitude $\langle\varphi\rangle(z) \Rightarrow \langle\varphi\rangle(\theta,\zeta):$

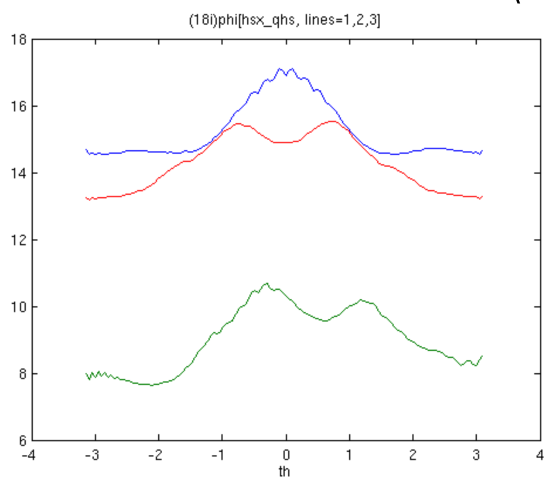

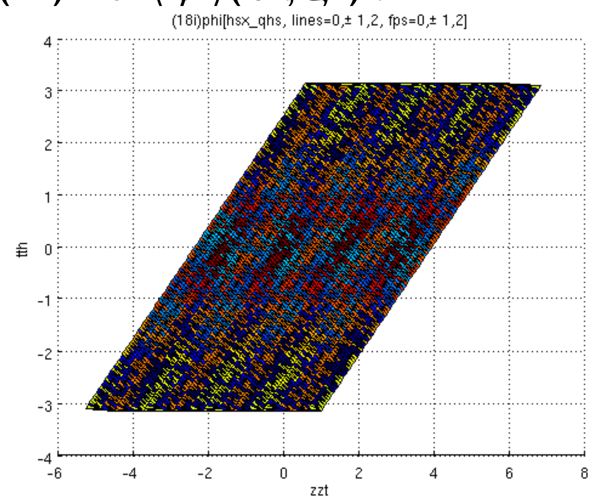

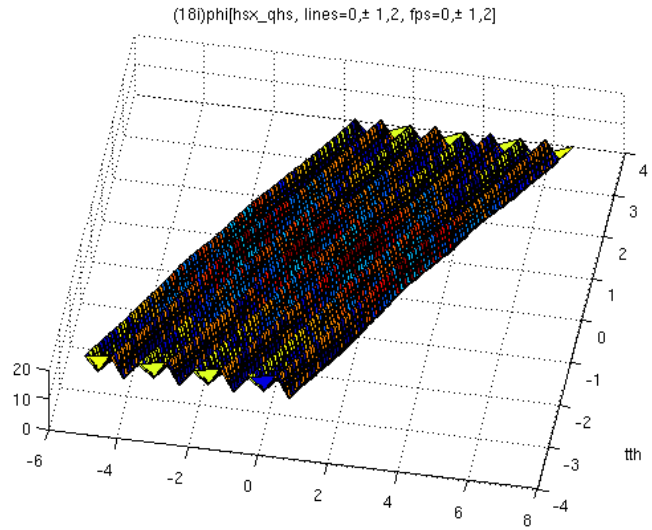

-radial curvature κ_1:

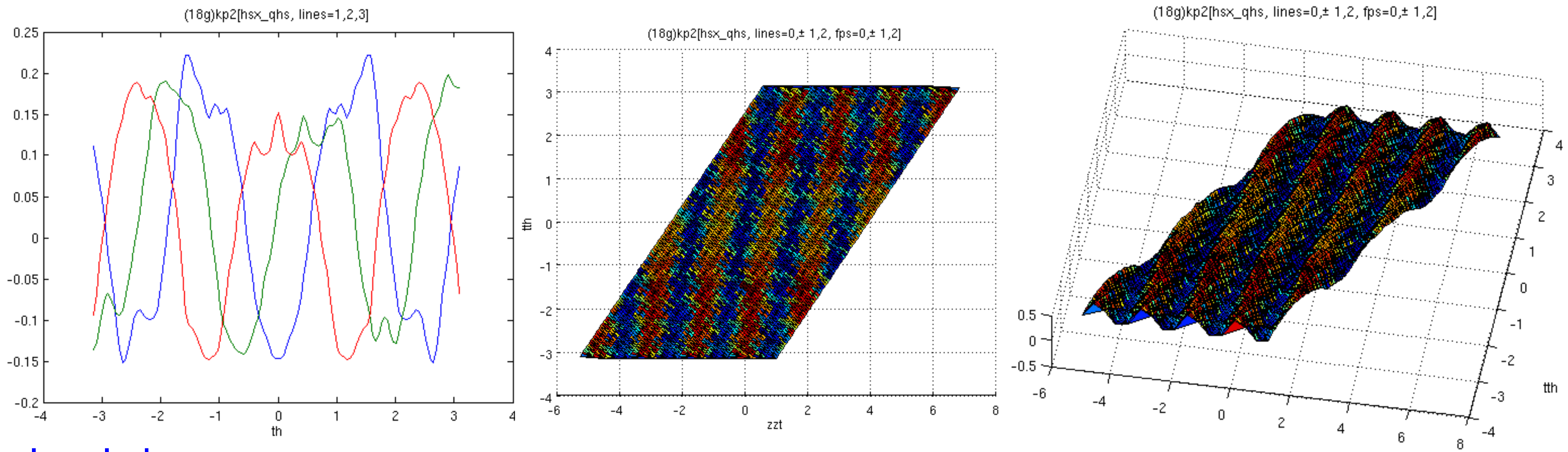

-local shear:

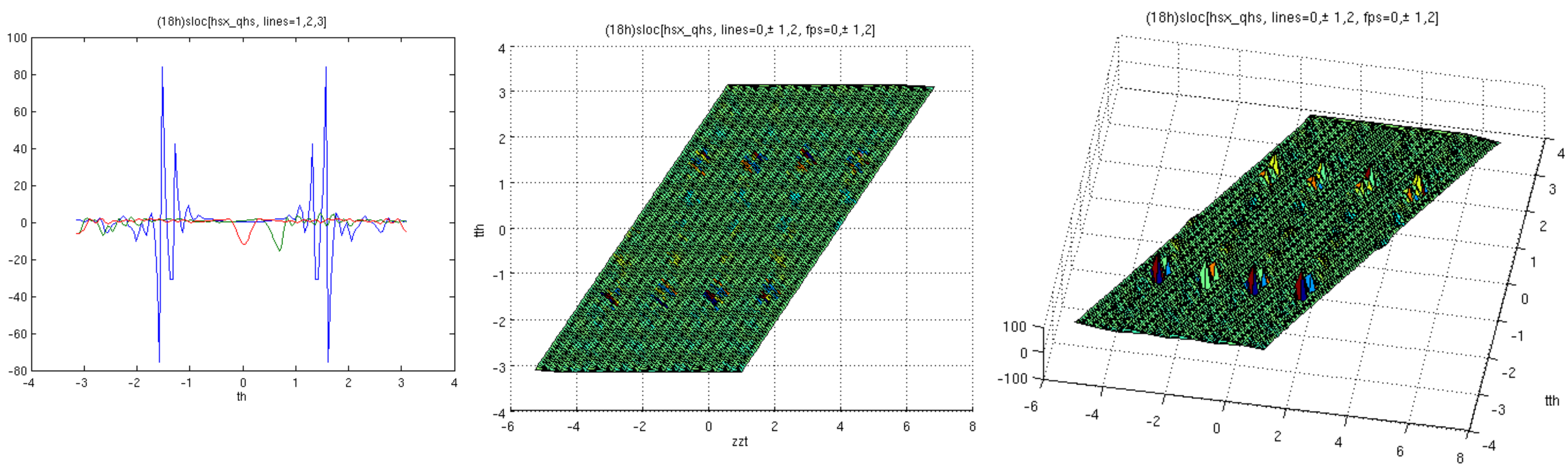

-Mode equation, effective potential V(θ) :

-Has been observed[3] that $\langle\varphi\rangle(\theta)$ for ITG turbulence resembles linear mode structure $\varphi_k(\theta) \rightarrow$ Consider dependence of $\varphi_k(\theta)$ via (ITG/TEM) linear mode eqn:

-From quasineutrality condition $0 = g_e/\tau + g_i,$ (4)

with $g_s = k^2\lambda_s^2(\text{susceptibility})$, have $g_e \xrightarrow{\text{adiabatic}} 1,$ (true for simulations here, so only ITG present in results)

$$g_i \simeq 1 - \left\langle J_0^2 \frac{\omega - \omega_{*i}^f}{\omega - k_\parallel v_\parallel - \omega_D} \right\rangle_v \simeq 1 + \left\langle J_0^2 \left(\frac{\omega_{*i}^f}{\omega} - 1 \right) \left[1 + \frac{\omega_d}{\omega} (\frac{u_\perp^2}{2} + u_\parallel^2) + \xi^{-2} u_\parallel^2 \right] \right\rangle_v \quad (5)$$

$$= c_0 + \omega^{-1} c_1 + \omega^{-2}[c_2 + d_2(qRk_\parallel)^2] + \omega^{-3} d_3 (qRk_\parallel)^2,$$

where $\langle A \rangle_v \equiv \int d\mathbf{v} A f_{s0}/n_{s0}, \xi \equiv \omega/(k_\parallel v_{Ti}), \omega_*^f \equiv \omega_*[1 + \eta(u^2 - 3)/2]$, with $\omega_* \equiv -ck_\theta \kappa_n T/(eB), \eta \equiv \kappa_T/\kappa_n,$ $\kappa_n \equiv 1/L_n \equiv -\partial_r n_0/n_0, \kappa_T \equiv 1/L_T \equiv -\partial_r T_i/T_i, \omega_D \equiv \mathbf{v}_D \cdot \mathbf{k} = \omega_d(u_\perp^2/2 + u_\parallel^2),$ $\omega_d \equiv cT_i/(e_i B^3)\mathbf{B} \times \nabla B \cdot \mathbf{k}_\perp = \rho_{gi} v_{Ti}(B/2L_\perp B_a)(k_1\kappa_1 + k_2\kappa_2)$, where $\kappa_1 \equiv -a\partial_y B/B$, and $\kappa_2 \equiv a\partial_x B/B, c_0 \equiv g_e/\tau + 1 - \Lambda_0(b_i), c_1 \equiv \ldots.$

Using $ik_\parallel \rightarrow \nabla_\parallel = (B\mathcal{J})^{-1}\partial_\theta = (B^\theta/B)\partial_\theta$, obtain mode equation

$$0 = [V(\theta) - (qRB^\theta/B)\partial_\theta(qRB^\theta/B)\partial_\theta)]\phi(\theta), \quad (6)$$

with effective potential $V(\theta|r, \theta_k, \omega) \equiv \dfrac{(\omega^2 c_0 + \omega c_1 + c_2)\omega}{\omega d_2 + d_3}.$ (7)

-Effective potential V for present family of configurations:

V[ncsx_sym]

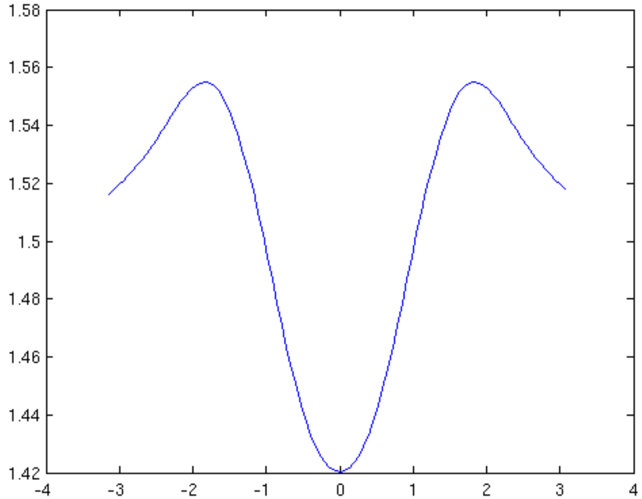

V[ncsx]

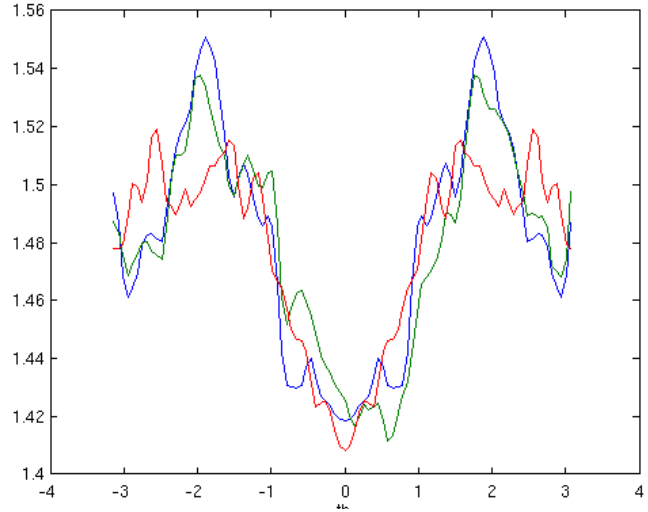

V[hsx]

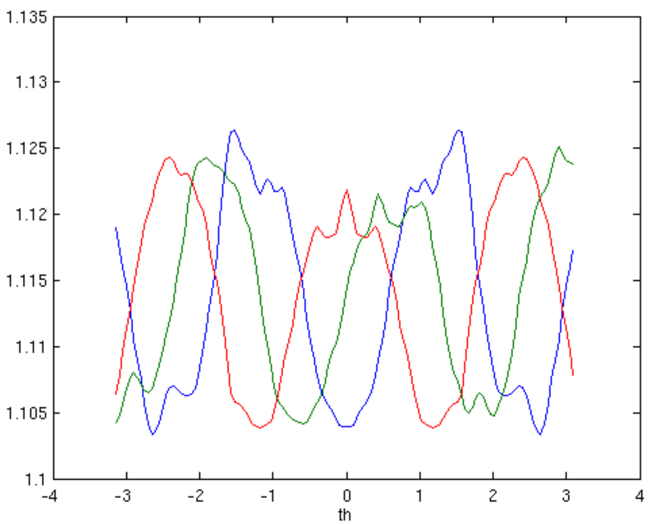

V[w7x]

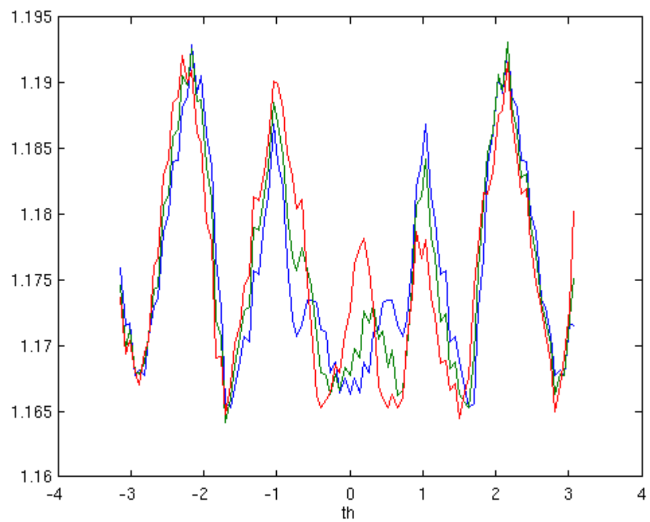

-Local shear $s_l = \partial_\theta (g^{xy} / g^{xx})$:

-Enters mode eqn through modifying both $k_\parallel(\theta)$ and $k_x^2(\theta)$, enhancing Landau damping and reducing mode radial extent, a function similar to that played by ZFs. Thus, spikes in s_l tend to bound modes.

-Examples: (a)NCSX,line-2. (b) Compare NCSX, line-0 with artificial configuration NCSX_s, from NCSX by doubling s_l, by doubling g^{xy} while adjusting g^{yy} to preserve constraint $(B/B_a)^2 = g^{xx} g^{yy} - (g^{xy})^2$, keeping $(B/B_a), g^{xx}$ unchanged.

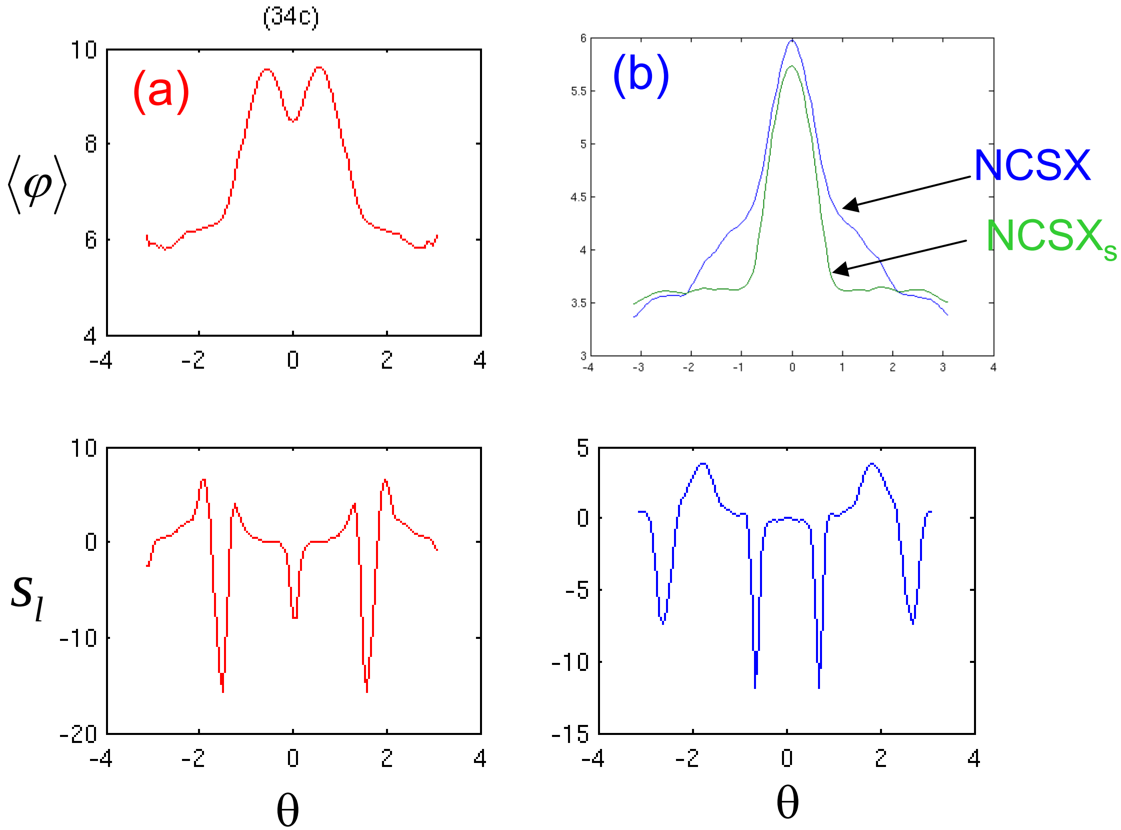

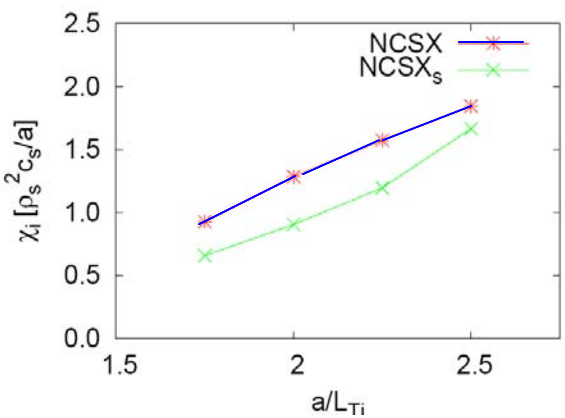

Transport reduced in NCSX_s by about 30%:

-Radial heat flux Q_i :

Strongly resembles the turbulent amplitude $\langle\varphi\rangle$,

with rough scaling $Q_i(z) \sim \left\langle | E_y |^2 \right\rangle \sim \sum_k k_y^2 \left\langle | \varphi_k |^2 \right\rangle$, suggesting weak turbulence:

-Eg:

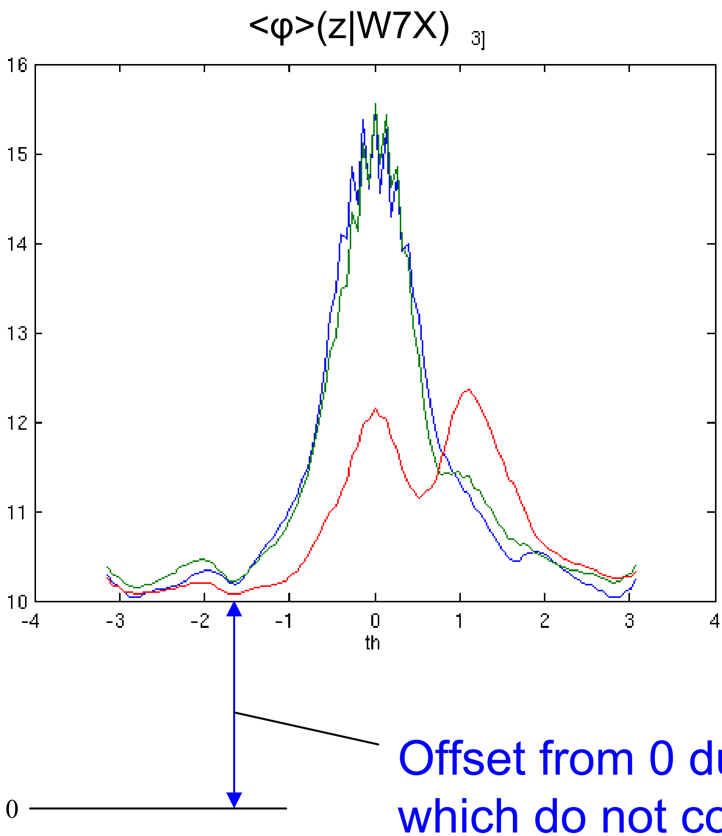

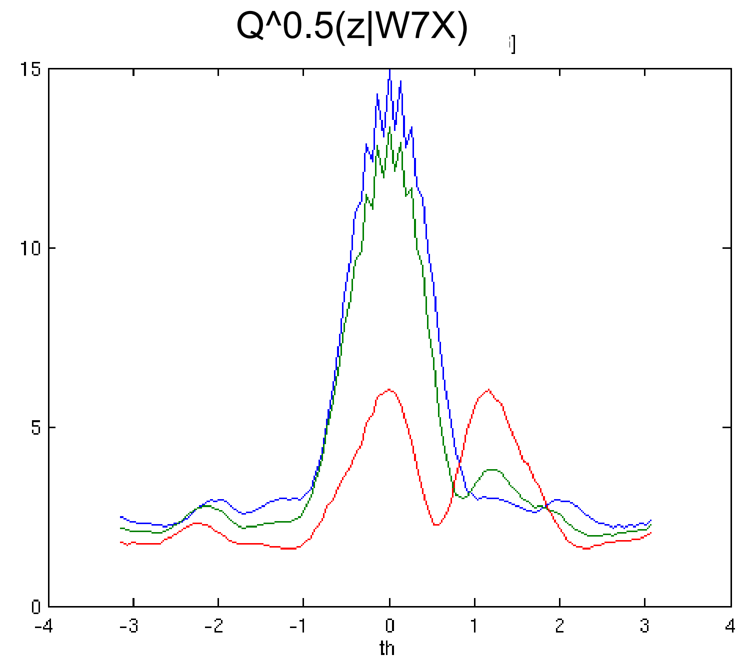

Offset from 0 due to low-k_y modes, mainly ZFs, which do not contribute to Q_i.

-Line-to-line variation of heat flux Q(t):

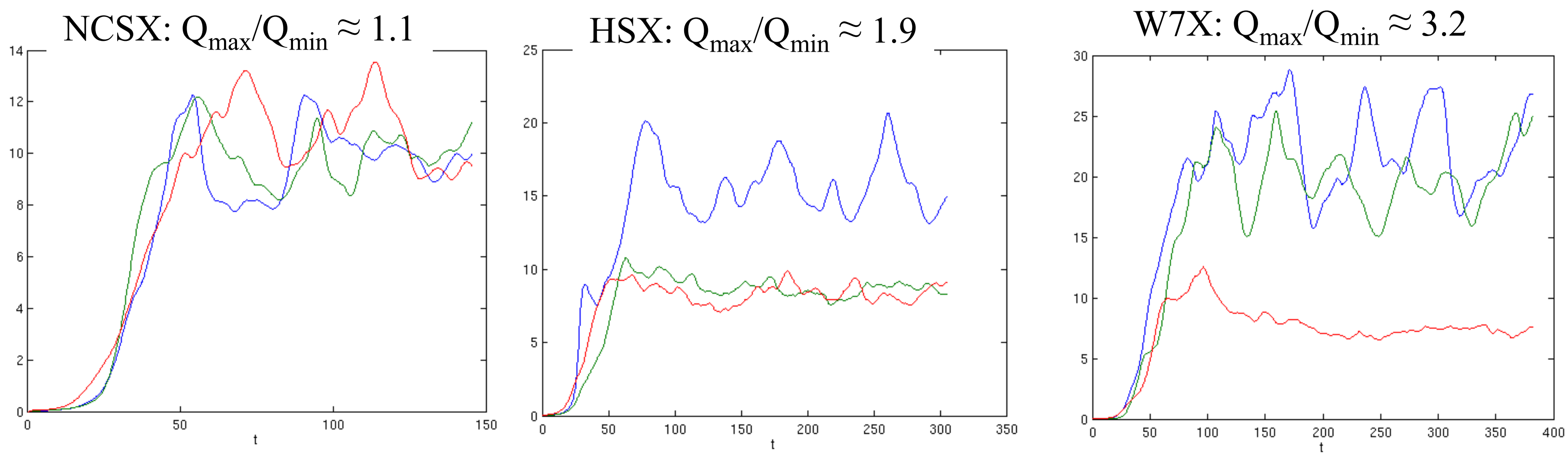

-Surface avging heat flux Q(t), find

<Q>(NCSX_sym : NCSX : HSX : W7X)

:: 7.9 : 9.9 : 10.4 : 17

-(These particular values may be expected to change with other profiles, and additional effects, such as kinetic electrons, ambipolar field, etc. Most noteworthy is that all are comparable to a 2D system, and to each other.)

-Apply neural networks (NNs) to GENE runs

to try to relate gk output (like $<\varphi>$, Q_i) to input quantities (like κ_1, s_l)
(by **L.Maingi**, H.Mynick, N.Pomphrey):

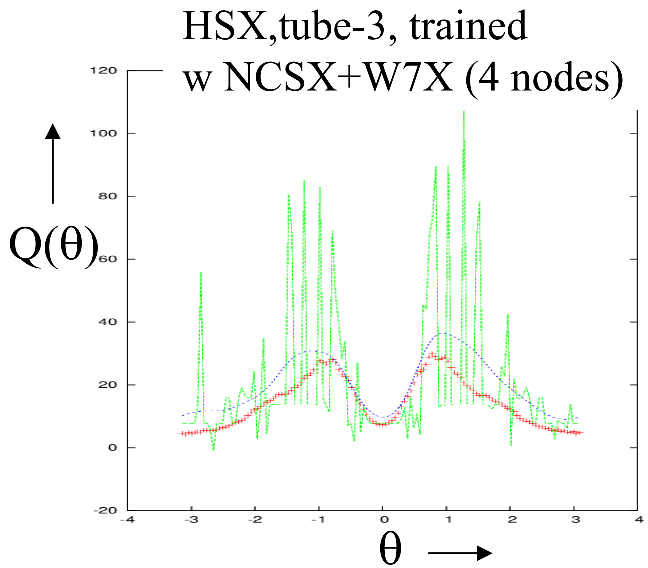

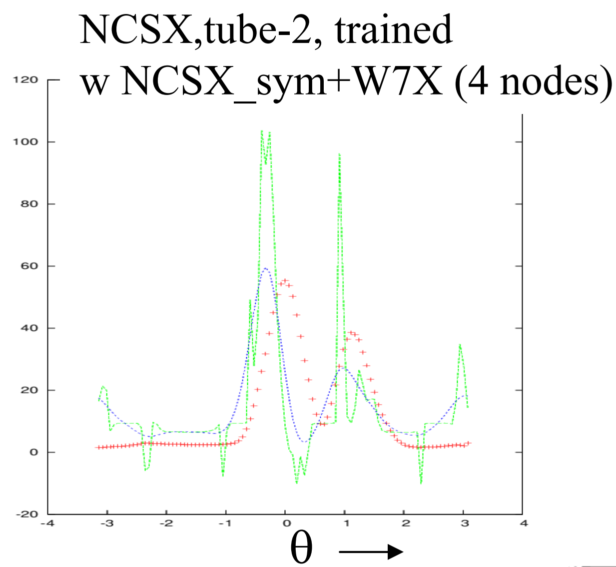

(**key:** red=GENE result,
green=raw NN,
blue=avged NN)

-From this, can construct 2D map of $Q_i(\kappa_1, s_l)$:

Q_i large where κ_1 large & <0, s_l ~ 0 ,
consistent with findings above.

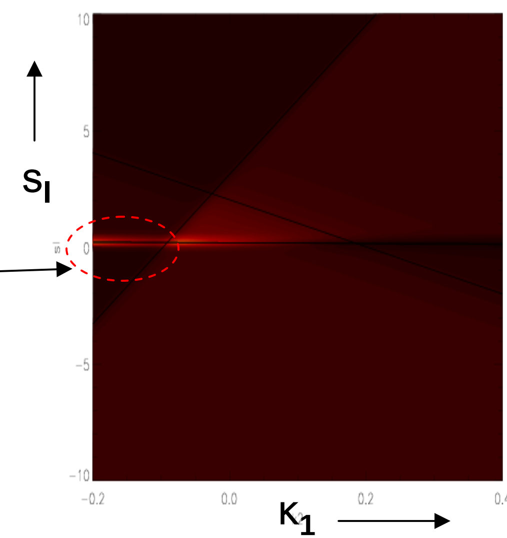

-Summary:

-Using the stellarator gk code GENE, have computed the turbulence & transport for a family of stellarators of widely-ranging designs, to understand the geometry-dependence of the turbulence.

-From the 1D flux-tube results, have constructed the 2D structure of the turbulence over a flux-surface, & related this to relevant geometric quantities, including the effective potential V(z) in the Schroedinger-like equation for linear drift modes.

- $\langle\varphi\rangle$ resembles the most unstable linear modes φ_k, localizing in the wells of V, where κ_1 is worst (most negative), occurring on the outboard side around the device corners (bean cross-section).

-Spatial form of heat flux $Q_i(z)$ resembles turbulent $\langle\varphi\rangle(z)$, with approximate scaling $Q_i(z) \sim \langle\varphi^2\rangle(z)$, suggesting weak turbulence.

-The form of V(z) is dominated by that of curvature $\kappa_1(z)$, from the drift term.

-For all systems, the ripple wells in V() on the helical (L_h)-scale are too short to localize $\langle\varphi\rangle$ (at least for the ITG turbulence simulated here), with the residual longer toroidal (L_t-scale) variation again causing ballooning toward θ=0.

-Spikes in local shear $s_l(z)$ tend to bound modes, through moving $k_\parallel(z)$ and $k_x^2(z)$ away from 0, suppressing $\langle\varphi\rangle$ and Q_i , thus playing a role similar to ZFs.

-The relatively simple relationship between GENE outputs $\langle\varphi\rangle$,Q_i and inputs like κ_1, s_l , which can be quickly computed, suggests an optimization may be done, minimizing a semi-analytic proxy $Q_i(\kappa_1, s_l)$ for the transport.

-References:

[1] F. Jenko et al., Phys. Plasmas **7** (2000)
[2]P. Xanthopoulos, F. Jenko, Phys.Plasmas **13**, 092301 (2006).
[3] P. Xanthopoulos, F.Merz, T.Goerler, F. Jenko, PRL **99**, 035002 (2007).
[4] G. Rewoldt, L.-P. Ku, W. M. Tang, Phys. Plasmas **12**, 102512 (2005)